

Systematics of the Multi-Regge Three-Loop Symbol

TILL BARGHEER

DESY Theory Group, DESY Hamburg, Notkestraße 85, D-22607 Hamburg, Germany

till.bargheer@desy.de

Abstract

We review the systematics of Mandelstam cut contributions to planar scattering amplitudes in the multi-Regge limit. Isolating the relevant cut terms, we explain how the BFKL expansion can be used to construct the perturbative n -point MHV multi-Regge limit symbol from a finite number of basic building blocks. At three loops and at leading logarithmic order, two building blocks are required. These are extracted from the known three-loop six-point and seven-point symbols for general kinematics. The subleading and sub-subleading terms require two and one further building block, respectively. The latter could either be reconstructed from further perturbative data, or from BFKL integrals involving yet-unknown corrections to the central emission vertex, on whose construction we also briefly comment.

Contents

1	Introduction	2
2	Background	3
3	Symbols and Regions	8
4	Two-Loop Expansion	10
5	Three-Loop Expansion	13
6	Building Blocks	16
7	Conclusion	17
	References	18

1 Introduction

Recent advances in the study of scattering amplitudes have sparked renewed interest in the multi-Regge limit of high-energy scattering. Besides its phenomenological significance, it has long been noted that the perturbative expansion simplifies considerably in this limit: Typically, the perturbative series has to be (and in fact can be!) resummed due to the appearance of large logarithms, leading to factorized all-order expressions for scattering processes. A further enhancement comes about in the case of planar $\mathcal{N} = 4$ super Yang–Mills theory: Here, the multi-Reggeon states that resum all-order gluon exchanges are governed by the integrable Balitsky–Fadin–Kuraev–Lipatov (BFKL) [1] and Bartels–Kwieciński–Praszałowicz (BKP) [2] Hamiltonians. This first appearance of integrability in the planar theory was observed long before the extensive discoveries and applications of integrable structures that took place during the past fifteen years [3]. Since the proposal of the exponentiated Bern–Dixon–Smirnov (BDS) amplitude [4], the systematics of multi-Regge limit amplitudes in planar $\mathcal{N} = 4$ super Yang–Mills theory have been understood to a remarkable extent. In fact, after a disagreement at strong coupling had casted doubt on the correctness of the BDS amplitude [5], it was the absence of the expected Regge pole and cut terms that invalidated the proposal at weak coupling [6], and that prompted the correction of the BDS amplitude by the dual conformally invariant remainder function beyond five points [7, 8].

By now, the remainder function has been constructed to high loop orders by constraining the possible function space through physical symmetry and analyticity requirements [9, 10]. This *bootstrap program* relies on various input, ranging from the mathematical theory of the relevant functions [11] to recursion relations [12] and the expansion around collinear limits as dictated by integrability [13, 14]. In all cases, knowledge about the multi-Regge limit has provided important boundary data to the bootstrap enterprise. Conversely, these recent methods admit to compute the BFKL data to unprecedented orders [9, 15, 16]. To date, this fruitful interplay has mostly been restricted to the six-point case. An extension to seven-point functions has been initiated recently [17]. Going to even higher points will require a better understanding of the relevant function space. It is conceivable that the Regge limit will again provide valuable boundary data in this regard.

It has been understood that obtaining the full analytic structure of multi-Regge limit amplitudes requires to analyze the amplitudes in all possible kinematic regions [18–21]. In fact, while the integrable structure at strong coupling becomes particularly amenable in the multi-Regge limit [22], a discrepancy with the expectation from weak coupling has been observed in one of the kinematic regions at seven points [23]. Recently, a systematic study of the n -point two-loop remainder function in all kinematic regions at weak coupling has been put forward [24]. The ability to study any number of points relied on the known two-loop *symbol* of the remainder function for all multiplicities [25]. Passing from polylogarithmic functions to their symbols constitutes a major simplification, both for the analysis of the relevant expressions and for the systematics of the multi-Regge limit.

The goal of the present work is two-fold: One aim is to understand the results of the previous study [24] from the perspective of Regge cut contributions. Secondly, we want to lift the analysis to the three-loop level. To this end, we first isolate the Regge cut contributions that contribute to a given region, and then expand the relevant contributions to the three-loop order. Judiciously grouping the resulting terms, we find that the n -point three-loop remainder function, at the symbol level, reduces to a linear combination of a handful of building block functions. At the symbol level, the building blocks required to reconstruct the n -point remainder function at leading logarithmic order can be extracted from the known perturbative data. Our results are assembled in a computer-readable file attached to this submission.

Overview. In Section 2, we aim to summarize the systematics of planar scattering amplitudes in the multi-Regge limit in a self-contained way. Section 3 highlights the simplifications and restrictions implied by passing from functions to symbols. In Section 4, we revisit the two-loop analysis of the multi-Regge limit remainder function from the Regge cut point of view. Section 5 extends the analysis to three loops, and we find that the remainder function can be decomposed into a few basic building blocks. The latter are discussed in Section 6, and Section 7 presents our conclusion.

2 Background

Multi-Regge Kinematics. The $2 \rightarrow (n-2)$ multi-Regge limit is the n -particle generalization of the simple $s \gg t$ Regge limit for $2 \rightarrow 2$ scattering. To describe a general amplitude, we will use the $(3n-10)$ independent Lorentz invariants

$$t_j \equiv q_j^2, \quad q_j \equiv p_2 + p_3 + \cdots + p_{j-1}, \quad j = 4, \dots, n, \quad (2.1)$$

$$s_j \equiv s_{j-1,j} \equiv (p_{j-1} + p_j)^2, \quad j = 4, \dots, n, \quad (2.2)$$

$$\eta_j \equiv \frac{s_j s_{j+1}}{(p_{j-1} + p_j + p_{j+1})^2}, \quad j = 4, \dots, n-1. \quad (2.3)$$

Here, p_1, \dots, p_n are the n external momenta. By convention, they are all incoming, but may have either energy sign. The $2 \rightarrow (n-2)$ multi-Regge limit is attained for

$$|s| \gg |s_4|, \dots, |s_n| \gg t_4, \dots, t_n, \quad (2.4)$$

where $s = (p_1 + p_2)^2$ is the total energy. See Figure 1 for an illustration of the kinematics. Many quantities in the multi-Regge limit only depend on the kinematics in the transverse space to the (p_1, p_2) plane. We hence define

$$p_j = \alpha_j p_1 + \beta_j p_2 + p_j^\perp, \quad p_1 \cdot p_j^\perp = p_2 \cdot p_j^\perp = 0, \quad j = 4, \dots, n-1, \quad (2.5)$$

and similarly for q_4, \dots, q_n . It is often convenient to switch to complex variables p_j, q_j whose real and imaginary parts equal the two components of the transverse momenta p_j^\perp and q_j^\perp , respectively:

$$p_j^\perp = (\Re(p_j), \Im(p_j)), \quad q_j^\perp = (\Re(q_j), \Im(q_j)). \quad (2.6)$$

Frequently used combinations of the transverse momenta are the complex anharmonic ratios

$$w_j = \frac{p_{j-1} q_{j+1}}{q_{j-1} p_j}, \quad j = 5, \dots, n-1. \quad (2.7)$$

Planar $\mathcal{N} = 4$ super Yang–Mills theory enjoys dual conformal invariance. Invariant quantities in this theory can thus only depend on conformally invariant cross ratios

$$U_{ij} \equiv \frac{x_{i+1,j}^2 x_{i,j+1}^2}{x_{ij}^2 x_{i+1,j+1}^2}, \quad 3 \leq |i-j| \leq n-2 \quad (2.8)$$

of the dual coordinates

$$p_j \equiv x_j - x_{j-1}, \quad x_{ij} = x_i - x_j. \quad (2.9)$$

A multiplicatively independent basis of invariant cross ratios is provided by

$$u_{j,1} = U_{j-2,j+1}, \quad u_{j,2} = U_{j-1,n}, \quad u_{j,3} = U_{1,j}, \quad j = 4, \dots, n-2. \quad (2.10)$$

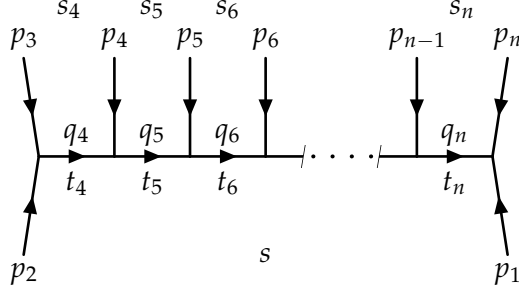


Figure 1: Kinematic variables.

In the multi-Regge limit, these cross ratios converge to 1 or 0:

$$u_{j,1} \rightarrow 1, \quad u_{j,2} \rightarrow 0, \quad u_{j,3} \rightarrow 0. \quad (2.11)$$

The ratios of subleading terms remain finite, and are related to the anharmonic ratios (2.7) via

$$\frac{u_{j,2}}{1 - u_{j,1}} \rightarrow \frac{1}{|1 + w_j|^2}, \quad \frac{u_{j,3}}{1 - u_{j,1}} \rightarrow \frac{|w_j|^2}{|1 + w_j|^2}. \quad (2.12)$$

Kinematic Regions. In order to understand the full analytic structure of the multi-Regge limit amplitude, it is important to analyze it in all physical kinematic regions. Our starting point will be the physical region in which the energies of all particles $3, \dots, n$ are negative (which means that those particles are effectively outgoing, instead of incoming). In this region, all subenergies s_j , $j = 4, \dots, n$, are negative.¹ In all other physical regions that we will consider, some of the particles $4, \dots, n-1$ have positive energies, and hence some of the invariants s_j become positive. These are sometimes called “Mandelstam regions”.² They can be reached from the all-negative region by analytic continuation of the kinematics. The various regions will be labeled by the subsets $I \subset \{4, \dots, n-1\}$ of particles whose energies have been continued to positive values. Alternatively, we will often label regions by $\rho = (\rho_4, \dots, \rho_{n-1}) \in \mathbb{Z}_2^{n-4}$, with $\rho_j = \pm 1$ (or just $\rho_j = \pm$) indicating the sign of the respective particle’s energy.

Importantly, the various regions become disconnected in the strict multi-Regge limit. That is to say, in order to continue the kinematics from one region to the other, one has to complexify the subenergies s_k (e.g. by continuing them along big circles).

Multi-Regge Limit Amplitudes. Scattering in the multi-Regge limit is dominated by the exchange of “Reggeized gluons” (or “Reggeons”), which are effective particles that resum the contributions of entire classes of gluonic Feynman diagrams of all loop orders. The simplest example is the four-point amplitude in *planar* $\mathcal{N} = 4$ super Yang–Mills theory,³ for which *all* perturbative contributions can resummed and factorized into a single diagram:

$$\mathcal{A}_4^{\text{MRL}} = \text{diagram} = \Gamma(t) s^{\omega(t)} \Gamma(t). \quad (2.13)$$

¹The Minkowski metric is assumed to have signature $(-+++)$.

²One could also consider regions in which the energies of particles 3 and/or n are positive, but those regions do not add further analytic structure to the amplitude, and will thus not be considered in the following.

³General non-planar amplitudes also receive contributions from multi-Reggeon exchanges; for the four-point and five-point amplitudes, these are suppressed by powers of $1/N_c$ in the planar limit.

Here, $\bullet = \Gamma(t)$ is the gluon-gluon-Reggeon vertex (see e.g. [6]), and --- stands for the exchange of a single Reggeon with propagator $s^{\omega(t)}$, where $\omega(t)$ is the (real-valued) Regge trajectory. At five points, two different kinematic regions can be considered: The produced particle 4 can either have positive energy (+) or negative energy (-). Strikingly, the factorization property of the four-point amplitude extends to this case: In both regions, the planar five-point amplitude again factorizes into a single diagram,

$$\mathcal{A}_5^{\text{MRL}(\pm)} = \begin{array}{c} \diagup \quad \diagdown \\ \bullet \text{---} \ominus \text{---} \bullet \\ \diagdown \quad \diagup \end{array} = \Gamma(t_4) s_4^{\omega(t_4)} \Gamma_{45} s_5^{\omega(t_5)} \Gamma(t_5), \quad (2.14)$$

where the (complex) gluon production vertex [8]

$$\begin{array}{c} j \\ \text{---} \oplus \text{---} \end{array} = \Gamma_{j,j+1} = |\Gamma_{j,j+1}| e^{\pm i\pi \hat{\omega}_{j,j+1}}, \quad \hat{\omega}_{j,j+1} = \hat{\omega}(t_j, t_{j+1}, \eta_j), \quad (2.15)$$

only depends on the kinematic region through the sign of its phase. A general multi-Regge-limit amplitude in any given kinematic region ρ receives contributions from Regge pole as well as Mandelstam cut terms,

$$\mathcal{A}_{n,\rho}^{\text{MRL}} = \mathcal{A}_{n,\rho}^{\text{Regge pole}} + \mathcal{A}_{n,\rho}^{\text{Mandelstam cut}}. \quad (2.16)$$

Both the pole terms and the cut terms depend on the kinematic region ρ . The origin of the Mandelstam cut terms are non-trivial contributions from multi-Reggeon bound state exchange in intermediate t -channels. For planar amplitudes of up to five points, such contributions are suppressed by powers of $1/N_c$, and the amplitudes factorize as indicated above. At six points, the first cut term appears, in the region $(++)$ where both intermediate momenta have been flipped [7]. In a generic region ρ , the six-point amplitude therefore reads [8,20]

$$\mathcal{A}_{6,\rho}^{\text{MRL}} = (\text{pole terms})^\rho + c_{6,1,4}^\rho \begin{array}{c} \diagup \quad \diagdown \\ \bullet \text{---} \square \text{---} \bullet \\ \diagdown \quad \diagup \end{array}, \quad (2.17)$$

where the region-dependent coefficient $c_{6,1,4}^\rho$ is non-vanishing for $\rho = (++)$. Here, the cut diagram stands for all contributions from two-Reggeon bound state exchange in the t_5 channel. This picture generalizes to higher multiplicities: The planar n -point multi-Regge limit amplitude is a sum of region-dependent Regge pole terms [26] as well as Mandelstam cut contributions [27,28] with region-dependent coefficients:

$$\begin{aligned} \mathcal{A}_{n,\rho}^{\text{MRL}} = & (\text{pole terms})^\rho + \sum_j c_{n,1,j}^\rho \begin{array}{c} j \\ \text{---} \text{---} \square \text{---} \text{---} \bullet \\ \diagdown \quad \diagup \end{array} + \sum_j c_{n,2,j}^\rho \begin{array}{c} j \\ \text{---} \text{---} \square \text{---} \square \text{---} \bullet \\ \diagdown \quad \diagup \end{array} + \dots \\ & + \sum_j d_{n,1,j}^\rho \begin{array}{c} j \\ \text{---} \text{---} \square \text{---} \square \text{---} \square \text{---} \bullet \\ \diagdown \quad \diagup \end{array} + \sum_j e_{n,j,k}^\rho \begin{array}{c} j \quad k \\ \text{---} \text{---} \square \text{---} \text{---} \square \text{---} \text{---} \bullet \\ \diagdown \quad \diagup \end{array} + \dots \quad (2.18) \end{aligned}$$

Here, the symbol --- stands for the insertion of zero or more complex gluon production vertices (2.15). For planar amplitudes, the number of exchanged Reggeons can at most increase or decrease by one when passing from one t -channel to the next.⁴ All other contributions are suppressed by powers of $1/N_c$. The pole terms as well as the cut-term prefactors

⁴The number M_n of admissible diagrams that can contribute to the n -point amplitude, as a sequence in n , equals the Motzkin sequence, OEIS A001006 [29], with $M_n/M_{n-1} \rightarrow 3$ for $n \rightarrow \infty$.

can in principle be obtained from the general quantum field theory principles of locality & unitarity. The procedure particularly relies on expanding the amplitude into a sum of terms that each have no overlapping energy discontinuities. Determining the cut contributions in this way is a very intricate and tedious procedure that has to be carried out region by region. This formidable task has been carried out for the seven-point amplitude [21], and a study of the eight-point case is underway [30], but a generalization to higher multiplicities appears difficult.

In fact, the *Mandelstam criterion* [28] significantly constrains the set of cut terms that can contribute to any given kinematic region: It asserts that any cut contribution in which the multi-Reggeon states span the adjacent t -channels t_j, \dots, t_k cannot contribute to regions in which $s_{j-1} > 0$ or $s_{k+1} > 0$, that is⁵

$$c_{n,k-j,j}^\rho = 0 \quad \text{if} \quad \rho_{j-1} = \rho_j \quad \text{or} \quad \rho_k = \rho_{k+1}, \quad (2.19)$$

and similarly for the further coefficients in (2.18). Here, the subscripts n, b , and j in $c_{n,b,j}^\rho$ label the total number of particles, the number of t -channels taking part in the multi-Reggeon state, and the produced gluon that bounds the multi-Reggeon state. As indicated above, the six-particle cut term (2.17) is only present in the $(++)$ region:

$$c_{6,1,4}^{(--)} = c_{6,1,4}^{(+-)} = c_{6,1,4}^{(-+)} = 0. \quad (2.20)$$

BDS and Remainder Function. The MHV amplitudes of planar $\mathcal{N} = 4$ super Yang–Mills theory can be decomposed into two factors:

$$\mathcal{A}_n^{\text{MHV}} = \mathcal{A}_n^{\text{BDS}} R_n \quad (2.21)$$

Here, $\mathcal{A}_n^{\text{BDS}}$ is the Bern–Dixon–Smirnov amplitude [4], which equals the tree-level amplitude times the exponentiated one-loop amplitude, and which in fact produces the correct all-loop four-point and five-point amplitudes. Starting at six points, it however fails to reproduce the correct Regge pole contributions, and it misses all Regge cut terms (beyond one loop) [6–8]. Hence it cannot be the full amplitude, but has to be corrected by a non-trivial *remainder function* R_n . Since the BDS amplitude correctly captures all infrared singularities and dual conformal weights, the remainder function is infrared finite and dual conformally invariant, and thus can only depend on dual conformally invariant cross ratios. By definition, it is only non-trivial starting from six points and two loops.

Passing to the multi-Regge limit, and stripping off the universal absolute value, a region-dependent phase factor remains. From the latter, one can separate off a conformally invariant, infrared finite part $\exp(i\delta_n^\rho)$, which again is region-dependent, and contains the finite part of the one-loop Regge cut terms [8, 20]

$$\frac{\mathcal{A}_n^{\text{BDS,MRL},\rho}}{\Gamma(t_4) |s_4^{\omega_4}| |\Gamma_{45}| |s_5^{\omega_5}| |\Gamma_{56}| |s_6^{\omega_6}| \dots |s_{n-1}^{\omega_{n-1}}| |\Gamma_{n-1,n}| |s_n^{\omega_n}| \Gamma(t_n)} = \exp(i\phi_n^\rho) \exp(i\delta_n^\rho). \quad (2.22)$$

The universal denominator is a generalization of the five-point amplitude (2.14), and it subsumes all dependence on the absolute values of the gluon production vertices $\Gamma_{k,k+1}$ and Reggeon propagators $s_k^{\omega_k}$. The region-dependent phase $e^{i\phi}$ absorbs the remaining infrared

⁵The reason is that in such cases, one of the Feynman loop integrals can be closed trivially, since all singularities lie on the same side of the integration contour [31].

divergences. The finite piece $e^{i\delta}$ combines in a non-trivial way with the remainder function to a region-dependent linear combination of reduced pole and cut terms [20]:

$$\begin{aligned}
\exp(i\delta_n^\rho) R_n^\rho &= (\text{reduced pole terms})^\rho \\
&+ \sum_j c_{n,1,j}^\rho \text{ [diagram 1] } + \sum_j c_{n,2,j}^\rho \text{ [diagram 2] } + \dots \\
&+ \sum_j d_{n,1,j}^\rho \text{ [diagram 3] } + \sum_{j < k} e_{n,j,k}^\rho \text{ [diagram 4] } + \dots
\end{aligned} \tag{2.23}$$

Here, the grayed-out parts of the cut diagrams have been divided out, and the (black) cut pieces stand for the remainder after the division.

Factorized Cut Integrals. All reduced cut terms in (2.23) are infrared-finite, conformally invariant functions of the complex anharmonic ratios w_k (2.7). Just like the pole terms of the four-point and five-point amplitudes, they enjoy the virtue of Regge factorization, in the following sense: The multi-Reggeon bound states that propagate in the intermediate t -channels are governed by the BFKL [1] and BKP [2] equations. The solutions to these equations are most naturally expressed in terms of their $SL(2, \mathbb{C})$ representation labels (n, ν) . Expressing all quantities in terms of these variables, the cut contribution factorizes into a simple product: Reading a cut diagram from left to right, each t -channel m -Reggeon state contributes one BFKL (or BKP) *Green's function* $G_m(n_k, \nu_k)$, each gluon emission that increments or decrements the number of exchanged reggeons from m to $m \pm 1$ contributes an *impact factor* $\Phi_{m,m\pm 1}(n_{k-1}, \nu_{k-1}, n_k, \nu_k)$, and each intermediate gluon k that gets emitted from an m -Reggeon bound state contributes a *central emission vertex* $C_m(n_{k-1}, \nu_{k-1}, n_k, \nu_k)$. Obtaining the full cut contribution requires completing the state sums in all t -channels by summing and integrating over all n_k and ν_k . The summation and integration amounts to a Fourier–Mellin transform from the (n_k, ν_k) variables to the complex anharmonic ratios w_k that provide the kinematic dependence.

The subsequent analysis will focus on the cuts of the type shown in the middle line of (2.23). For those terms, only the simplest impact factors [7]

$$\begin{aligned}
\Phi_{L,k} &\equiv \Phi_{0,1}(n_k, \nu_k) = \frac{1}{2} \frac{(-1)^n}{i\nu_k + n_k/2} \left(\frac{q_{k-1}}{p_{k-1}} \right)^{-i\nu_k - n_k/2} \left(\frac{\bar{q}_{k-1}}{\bar{p}_{k-1}} \right)^{-i\nu_k + n_k/2} + \mathcal{O}(g), \\
\Phi_{R,k} &\equiv \Phi_{1,0}(n_k, \nu_k) = -\frac{1}{2} \frac{1}{i\nu_k - n_k/2} \left(\frac{q_{k+1}}{p_k} \right)^{i\nu_k + n_k/2} \left(\frac{\bar{q}_{k+1}}{\bar{p}_k} \right)^{i\nu_k - n_k/2} + \mathcal{O}(g)
\end{aligned} \tag{2.24}$$

and emission vertices [19]

$$\begin{aligned}
C_k &\equiv C_1(n_k, \nu_k, n_{k+1}, \nu_{k+1}) = -\frac{1}{2} \left(\frac{q_{k+1}}{p_k} \right)^{i\nu_k + n_k/2} \left(\frac{\bar{q}_{k+1}}{\bar{p}_k} \right)^{i\nu_k - n_k/2} \\
&\cdot \left(\frac{q_k}{p_k} \right)^{-i\nu_{k+1} - n_{k+1}/2} \left(\frac{\bar{q}_k}{\bar{p}_k} \right)^{-i\nu_{k+1} + n_{k+1}/2} \tilde{C}(n_k, \nu_k, n_{k+1}, \nu_{k+1}) + \mathcal{O}(g)
\end{aligned} \tag{2.25}$$

are needed. The required Green's function stems from the BFKL color-octet channel and takes the form [7]

$$G_k \equiv G_2(n_k, \nu_k) = \varepsilon_k^{g E_{n_k, \nu_k}}. \quad (2.26)$$

Here, $\varepsilon_k \equiv -\sqrt{u_{k,2} u_{k,3}}$ are combinations of "small" cross ratios (2.10) that approach zero in the multi-Regge limit, $E_{n,\nu}$ is the BFKL color-octet eigenvalue, and

$$g \equiv \frac{g_{\text{YM}}^2 N_c}{8\pi^2} \quad (2.27)$$

is the planar coupling constant. The general two-Reggeon cut term f_k spanning k t -channels therefore takes the form [19, 23]⁶

$$f_k(\varepsilon_5, \dots, \varepsilon_{k+4}; w_5, \dots, w_{k+4}) \equiv \begin{array}{c} 4 \qquad \qquad \qquad k+4 \\ \text{---} \text{---} \text{---} \text{---} \text{---} \text{---} \\ \text{---} \text{---} \text{---} \text{---} \text{---} \text{---} \\ \text{---} \text{---} \text{---} \text{---} \text{---} \text{---} \end{array} = i g \sum_{n_5, \dots, n_{k+4}} \int d\nu_5 \dots d\nu_{k+4} \Phi_{L,5} \varepsilon_5^{g E_{n_5, \nu_5}} C_5 \varepsilon_6^{g E_{n_6, \nu_6}} C_6 \dots C_{k+3} \varepsilon_{k+4}^{g E_{n_{k+4}, \nu_{k+4}}} \Phi_{R, k+4}. \quad (2.28)$$

One can see that the exponentials of kinematic variables in the impact factors and emission vertices indeed combine into Fourier–Mellin integral transformation kernels

$$w_k^{i\nu_k + n_k/2} \bar{w}_k^{i\nu_k - n_k/2} = \rho_k^{2i\nu_k} e^{in_k \varphi_k} \quad \text{for} \quad w_k = \rho_k e^{i\varphi_k}. \quad (2.29)$$

Perturbative Expansion. The expression (2.28) is valid to all orders in the coupling g , where all coupling dependence is contained in the impact factors $\Phi_{L,R}$, the emission vertices C_k , and the BFKL eigenvalues E_{n_k, ν_k} . Upon a perturbative expansion, the BFKL Green's functions (2.26) expand in powers of g and of $\log(\varepsilon_k)$; the latter are the large logarithms that are characteristic of the multi-Regge limit. Including subleading terms of the BFKL eigenvalues, impact factors, and emission vertices, the cut contribution (2.28) at each order g^ℓ in the coupling constant becomes a polynomial of degree $(\ell - 1)$ in the large logarithms $\log \varepsilon_k$. Retaining only the leading terms in large logarithms amounts to the leading logarithmic approximation (LLA), the first subleading terms constitute the next-to-leading logarithmic approximation (NLLA), and so on. At order g^ℓ , there are LLA terms of order $\log(\varepsilon_k)^{\ell-1}$ all the way to $N^{\ell-1}$ LLA terms of order $\log(\varepsilon_k)^0$. At a given loop order, the coefficient of each monomial in $\log(\varepsilon_k)$ is a function of the kinematics that exclusively depends on the complex anharmonic ratios w_k (2.7).

3 Symbols and Regions

Transcendentality and Symbols. Scattering amplitudes in planar $\mathcal{N} = 4$ super Yang–Mills theory display the property of uniform (or maximal) transcendentality, which means that every term in the ℓ -loop amplitude has the same transcendentality (or transcendental weight) 2ℓ . This concept relies on the assumption that the amplitude can be expanded in products of multiple polylogarithms (iterated integrals over $d \log$ integrands, MPLs for short) times zeta values times rational numbers.⁷ Every m -fold iterated integral is assigned transcendentality

⁶The cut contribution is normalized such that the cut coefficient $c_{6,1,4}^{\rho=(++)}$ of the six-point remainder function becomes unity. This choice differs from the normalization used in [21] by a factor of $2i$.

⁷It is expected that this class of functions is not sufficient to describe all amplitudes to all orders in general kinematics. For example, elliptic integrals appear in the ten-point N^3 MHV amplitude [32]. However, it appears conceivable that multiple polylogarithms suffice to describe all amplitudes in the multi-Regge limit. In any case, all quantities considered in this work are expressible in terms of polylogarithms.

m . Zeta values can be defined as MPLs evaluated on certain values, and they inherit the transcendentality of their parent functions. For example, the polylogarithms $\text{Li}_m(x)$ as well as the zeta values ζ_m have transcendentality m . Under multiplication, transcendentality behaves additively.

Multiple polylogarithms obey many functional identities, which makes them unwieldy, especially in expressions with many terms. All such functional relations trivialize when one projects all MPLs to their *symbols*.⁸ The latter discard all information contained in the choice of integration base point. In particular, the symbols are agnostic of all ambiguities lying in the choice of functional branch. Since all branch ambiguities of MPLs have subleading *functional* transcendentality (transcendentality of functional origin, as opposed to numerical transcendentality), one typically discards *all* terms of subleading functional transcendentality when mapping an expression to its symbol.

When projecting the amplitude to its symbol, the expression (2.23) simplifies considerably: The reduced pole terms consist of trigonometric functions whose arguments include factors of π [20,21], hence their perturbative expansion contains extra powers of $\pi = \zeta_2$, which implies that they carry subleading functional transcendental weight; they therefore get discarded. Cut terms that involve more than two Reggeons stem from double (or higher) discontinuities, hence they also have subleading transcendentality and get projected out. Terms with multiple disconnected multi-Reggeon states (such as the last term in (2.23)) are products of lower-loop cut terms, hence also these have subleading transcendental weight and get discarded. On the left hand side of the equation, the factor $e^{i\delta}$ can be truncated to 1, since all higher terms again include additional factors of π . In summary, at the level of the symbol:

$$R_n^\rho \simeq \sum_j c_{n,1,j}^\rho \left[\text{diagram} \right] + \sum_j c_{n,2,j}^\rho \left[\text{diagram} \right] + \dots \quad (3.1)$$

Here, “ \simeq ” denotes equality at the symbol level. Moreover, here and in the following, the remaining (black) cut pieces are understood to be one-loop subtracted, as the one-loop part is (by definition) contained in the BDS factor that has been divided out.

Symbols and Regions. The discontinuity of a symbol along a continuation path only depends on the overall winding numbers of the path around the singular points of the integrand. From this property alone, it follows [24] that the symbols $S[\cdot]$ of the multi-Regge-limit remainder function in the various kinematic regions obey the relations

$$S[R_n]_I^{\text{MRL}} = \sum_{\{k,l\} \subset I} S[R_n]_{\{k,l\}}^{\text{MRL}}. \quad (3.2)$$

and

$$S[R_n]_{\{k,l\}}^{\text{MRL}} = S[R_n]_{[k,l]}^{\text{MRL}} - S[R_n]_{[k,l-1]}^{\text{MRL}} - S[R_n]_{[k+1,l]}^{\text{MRL}} + S[R_n]_{[k+1,l-1]}^{\text{MRL}}. \quad (3.3)$$

These relations hold independently of the loop order. The first relation states that the symbol in any region $I \subset \{4, \dots, n-1\}$ is a sum of symbols in regions $\{k,l\}$ where only two momenta p_k and p_l are flipped. The second relation in turn expresses the symbol in those two-flip regions as a linear combination of symbols in regions where all flipped momenta k, \dots, l are adjacent, labeled by $[k,l]$. It is therefore sufficient to consider the symbol in those all-adjacent regions.

⁸See e.g. [33].

Note that, since the cut terms can be assumed to be functionally independent, the relations (3.2,3.3) among symbols imply identical relations for the cut prefactors $c_{n,b,j}^\rho$ in the various regions:

$$c_{n,b,j}^I = \sum_{\{k,l\} \subset I} c_{n,b,j}^{\{k,l\}}, \quad c_{n,b,j}^{\{k,l\}} = c_{n,b,j}^{[k,l]} - c_{n,b,j}^{[k,l-1]} - c_{n,b,j}^{[k+1,l]} + c_{n,b,j}^{[k+1,l-1]}. \quad (3.4)$$

It is not difficult to see that these relations are consistent with the Mandelstam criterion described above. They completely determine all simple two-Reggeon cut contributions of the type shown in (3.1) to the n -point remainder function in any kinematic region ρ , once the coefficients $c_{n,b,j}^{[k,l]}$ have been fixed.

In fact, the Mandelstam criterion implies that the only simple two-Reggeon cut contribution to the n -point multi-Regge limit remainder function in any all-adjacent region $[k, l]$ is the following:

$$R_n^{[k,l]} \simeq c_{n,l-k,k}^{[k,l]} \left(\text{diagram with } k \text{ and } \ell \text{ vertices} \right), \quad (3.5)$$

where “ \simeq ” again denotes equality at the symbol level, and the dots stand for the omission of $(l - k - 2)$ production vertices. In other words,

$$c_{n,b,j}^{[k,l]} = 0 \quad \text{unless} \quad j = k, \quad \text{and} \quad b = l - k. \quad (3.6)$$

In particular, all such symbols equal (up to variable substitution and the prefactors) the symbol of the $(l - k + 5)$ -point remainder function in the region where *all* intermediate momenta are flipped:

$$S[R_n]_{[k,l]}^{\text{MRL}}(\varepsilon_{k+1}, \dots, \varepsilon_l; w_{k+1}, \dots, w_l) = \frac{c_{n,l-k,k}^{[k,l]}}{c_{n',n'-4,4}^{[k,l]}} S[R_{n'}]_{[4,n'-1]}^{\text{MRL}}(\varepsilon_{k+1}, \dots, \varepsilon_l; w_{k+1}, \dots, w_l), \quad (3.7)$$

with $n' = l - k + 5$.

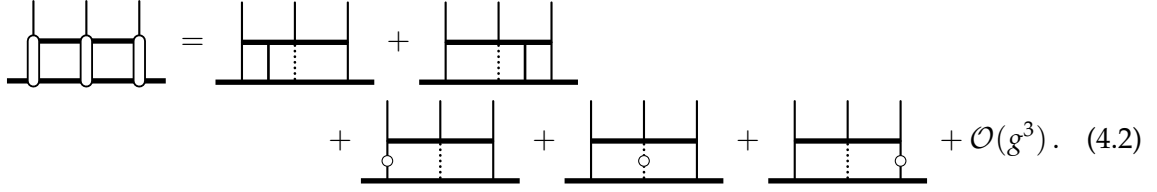
4 Two-Loop Expansion

We now want to analyze the simple two-Reggeon contribution (3.5) for any number of gluons at the perturbative level. The following deconstruction is not restricted to symbols, but holds at the level of full functions. By definition, we understand all cut diagrams of the type (3.5) to be one-loop subtracted. The simplest case involves only two emitted gluons. Perturbatively expanding the BFKL Green's function and the impact factors, the simplest diagram consists of three terms at the two-loop level:

$$\left(\text{diagram with loop} \right) = \left(\text{diagram with loop and dots} \right) + \left(\text{diagram with loop and dot} \right) + \left(\text{diagram with loop and dot} \right) + \mathcal{O}(g^3). \quad (4.1)$$

Here, a vertical line in the t -channel two-Reggeon state stands for the one-loop (order g^1) piece of the BFKL Green's function (2.26). In diagrams with no line insertions, the Green's function is trivial, $G_2(g = 0) = 1$. A naked line for the impact factor stands for its leading contribution (2.24), whereas additional dots denote loop corrections. The one-loop Green's function contains a factor $\log(\varepsilon_5)$, hence the first term provides the leading logarithmic

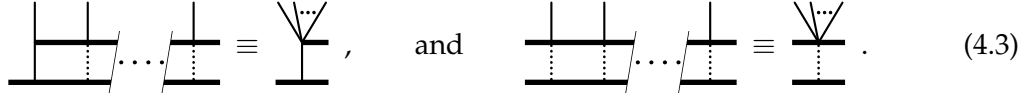
approximation (LLA) at this loop order. The subleading NLLA contribution consists of the second and third terms. Turning to the longer cut that appears in the (+++) region of the seven-point remainder function, the two-loop expansion yields five terms,



$$\begin{aligned}
& \text{Diagram 1} = \text{Diagram 2} + \text{Diagram 3} \\
& \quad + \text{Diagram 4} + \text{Diagram 5} + \mathcal{O}(g^3). \quad (4.2)
\end{aligned}$$

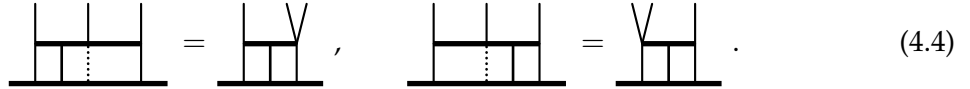
Here, the emission vertex makes its first appearance. Plain dotted lines stand for its leading term (2.25), and loop corrections are again denoted by dots. The LLA piece now consists of two terms, where either of the Green's functions in the first or second t -channel have been expanded to one-loop order. Hence the first term is proportional to $\log(\varepsilon_5)$, while the second term is proportional to $\log(\varepsilon_6)$. The second line provides the three NLLA terms.

A key fact for the subsequent analysis is the following observation [19]: Any number of adjacent leading-order production vertices, not separated by BFKL kernel insertions, can be absorbed in a neighboring leading-order impact factor (again not separated by BFKL kernel insertions). The result is the original impact factor, whose momentum gets replaced by the sum of combined momenta. Similarly, any number of adjacent leading-order production vertices can be combined into a multi-gluon production vertex, whose functional form is identical to the single-gluon vertex, but whose outgoing momentum is replaced by the sum of all combined momenta. Diagrammatically, we will denote these identities as



$$\begin{aligned}
& \text{Diagram 1} \dots \text{Diagram 2} \equiv \text{Diagram 3}, \quad \text{and} \quad \text{Diagram 4} \dots \text{Diagram 5} \equiv \text{Diagram 6}. \quad (4.3)
\end{aligned}$$

Here, the dots stand for the emission of any number of leading-order production vertices. Using these identities, one can reduce almost all diagrams in (4.2) to six-point diagrams. For example,



$$\begin{aligned}
& \text{Diagram 1} = \text{Diagram 2}, \quad \text{Diagram 3} = \text{Diagram 4}. \quad (4.4)
\end{aligned}$$

Each term in the two-loop expression (4.2) *a priori* depends on both complex anharmonic ratios w_5 and w_6 (2.7). But due to the identity (4.4), it is clear that all dependence of the first term in (4.2) on w_5 and w_6 factors into a dependence on the single complex ratio

$$v_{5,6;5} \equiv \frac{p_4 q_7}{q_4(p_5 + p_6)} = \frac{w_5}{(1 + \frac{1}{w_6})}. \quad (4.5)$$

Similarly, the second term in (4.2) only depends on the single complex ratio

$$v_{5,6;6} \equiv \frac{(p_4 + p_5)q_7}{q_4 p_6} = (1 + w_5)w_6. \quad (4.6)$$

Restricting to the LLA (the first line in (4.2)), and using the identities (4.4), the three-particle cut therefore reduces to a sum of two copies of the two-particle cut,

$$f_{2,(2)}^{\text{LLA}}(\varepsilon_5, \varepsilon_6; w_5, w_6) = f_{1,(2)}^{\text{LLA}}(\varepsilon_5; v_{5,6;5}) + f_{1,(2)}^{\text{LLA}}(\varepsilon_6; v_{5,6;6}). \quad (4.7)$$

Promoting this equation to the full two-loop cut contribution (including the NLLA piece) requires adding an extra NLLA term to the equation:

$$f_{2,(2)}(\varepsilon_5, \varepsilon_6; w_5, w_6) = f_{1,(2)}(\varepsilon_5; v_{5,6;5}) + f_{1,(2)}(\varepsilon_6; v_{5,6;6}) + g_2(v_{5,6;5}, v_{5,6;6}), \quad (4.8)$$

where

$$g_2(v_{5,6;5}, v_{5,6;6}) = \text{Diagram 1} - \text{Diagram 2} - \text{Diagram 3} \quad (4.9)$$

is a finite function of $v_{5,6;5}$ and $v_{5,6;6}$ (or of w_4 and w_5 via the relations (4.5,4.6)). Here, the last two terms are, by analogy with (4.3) defined by evaluating the one-loop impact factors on the sums of momenta $p_4 + p_5$ and $p_5 + p_6$, respectively.

This two-loop analysis straightforwardly generalized to the cut contribution for any number of particles. Using the identities (4.3), the LLO part of the general cut at two loops can be written as

$$f_{k,(2)}^{\text{LLA}}(\varepsilon_5, \dots, \varepsilon_{4+k}; w_5, \dots, w_{4+k}) = \sum_{j=5}^{4+k} \text{Diagram} = \sum_{j=5}^{4+k} f_{1,(2)}^{\text{LLA}}(\varepsilon_j; v_{5,4+k;j}). \quad (4.10)$$

Here, the variables

$$v_{k,l;j} \equiv \frac{q_{k-1} - q_j}{q_{k-1}} \frac{q_{l+1}}{q_j - q_{l+1}} = \frac{(1 + (1 + (\dots (1 + w_k)w_{k+1}) \dots)w_{j-1})w_j}{1 + \left(1 + \left(\dots \left(1 + \frac{1}{w_l}\right) \frac{1}{w_{l-1}}\right) \dots\right) \frac{1}{w_{j+1}}} \quad (4.11)$$

for $j = k, \dots, l$ are anharmonic ratios that generalize (4.5,4.6); they are obtained by grouping the adjacent momenta p_{k-1}, \dots, p_{j-1} and p_j, \dots, p_l . The inversion of this formula is much simpler,

$$w_j = \frac{(v_{k,l;j-1} - v_{k,l;j})(1 + v_{k,l;j+1})}{(1 + v_{k,l;j-1})(v_{k,l;j} - v_{k,l;j+1})}, \quad (4.12)$$

assuming the boundary conditions $v_{k,l;k-1} = 0$ and $v_{k,l;l+1} = \infty$. Including the NLO terms of $f_{k,(2)}$ and $f_{1,(2)}$ on both sides of equation (4.10), and again applying the reduction identities (4.3), one can see that all subleading terms combine into a sum of seven-point NLO pieces g_2 (4.9), evaluated with different complex ratios:

$$f_{k,(2)}(\varepsilon_5, \dots, \varepsilon_{4+k}; w_5, \dots, w_{4+k}) = \sum_{j=5}^{4+k} f_{1,(2)}(\varepsilon_j; v_j) + \sum_{j=5}^{3+k} g_2(v_j, v_{j+1}), \quad v_j \equiv v_{5,4+k;j}. \quad (4.13)$$

This concludes the two-loop analysis of the simple two-Reggeon cut (3.5). For any number of emitted particles, the latter can be deconstructed into a sum of two building blocks, one of them being the simplest two-particle cut f_1 , the other being the NLO remainder g_2 of the three-particle cut f_2 .

Using equation (3.5), the result (4.13) directly implies an analogous relation for the two-loop remainder function symbol in the region $(++ \dots +)$ where all momenta have been flipped,

$$R_{n,(2)}^{\text{MRL}}(\varepsilon_5, \dots, \varepsilon_{n-1}; w_5, \dots, w_{n-1}) \simeq \frac{c_n}{c_6} \sum_{j=5}^{n-1} R_{6,(2)}^{\text{MRL}}(\varepsilon_j; v_j) + c_n \sum_{j=5}^{n-2} g_2(v_j, v_{j+1}), \quad (4.14)$$

with the abbreviations $c_n \equiv c_{n,n-5,4}^{[4,n-1]}$ and $v_j \equiv v_{5,n-1;j}$. With the help of (3.7), very similar relations hold for the symbol in any region $[k, l]$ where any number of adjacent momenta have been flipped.

Relation to Previous Work. At leading logarithmic order, the relation (4.13) had been obtained before [19]. Here, we have generalized it to the full two-loop level, including the NLL0 terms. In fact, an explicit study [24] of the known two-loop symbol [25] has led to the slightly stronger observation

$$R_{n,(2)}^{\text{MRL}}(\varepsilon_5, \dots, \varepsilon_{n-1}; w_5, \dots, w_{n-1}) \simeq \sum_{j=5}^{n-1} R_{6,(2)}^{\text{MRL}}(\varepsilon_j; v_j) + c_7 \sum_{j=5}^{n-2} g_2(v_j, v_{j+1}). \quad (4.15)$$

Also this result had been obtained before at leading logarithmic order [34]. Comparing (4.14) with (4.15), one finds that the coefficients of all simple two-Reggeon cut contributions must be identical,⁹

$$c_{n,l-k,k}^{[k,l]} = c_{6,1,4}^{[4,5]} = 1, \quad n \geq 7, \quad 4 \leq k < l < n. \quad (4.16)$$

Here, the second equality follows from the deliberate choice of normalization (2.28) for the cut integral.

5 Three-Loop Expansion

We are now in a position to extend the previous analysis to the three-loop order. At three loops, the simplest cut contribution f_1 expands to

$$f_{1,(3)} = \begin{array}{c} \text{---} \text{---} \text{---} \text{---} \text{---} \\ | \quad | \quad | \quad | \quad | \\ \text{---} \end{array} + \begin{array}{c} \text{---} \text{---} \text{---} \text{---} \text{---} \\ | \quad | \quad | \quad | \quad | \\ \text{---} \end{array} + \begin{array}{c} \text{---} \text{---} \text{---} \text{---} \text{---} \\ | \quad | \quad | \quad | \quad | \\ \text{---} \end{array} + \begin{array}{c} \text{---} \text{---} \text{---} \text{---} \text{---} \\ | \quad | \quad | \quad | \quad | \\ \text{---} \end{array} \\ + \begin{array}{c} \text{---} \text{---} \text{---} \text{---} \text{---} \\ | \quad | \quad | \quad | \quad | \\ \text{---} \end{array} + \begin{array}{c} \text{---} \text{---} \text{---} \text{---} \text{---} \\ | \quad | \quad | \quad | \quad | \\ \text{---} \end{array} + \begin{array}{c} \text{---} \text{---} \text{---} \text{---} \text{---} \\ | \quad | \quad | \quad | \quad | \\ \text{---} \end{array}. \quad (5.1)$$

Compared to the two-loop case, there are a few new ingredients at three loops: Two line insertions in the two-Reggeon state (as in the first term) stand for terms where the BFKL Green's function (2.26) has been expanded to second order in the coupling g , while the BFKL eigenvalue $E_{n,v}$ has been kept at leading order. A line insertion dressed with a dot stands for one power of the one-loop correction to the eigenvalue $E_{n,v}$. Each line (leading order or loop corrected) comes with one power of the respective large logarithm $\log(\varepsilon_k)$. In other words, expanding

$$G_2(n_k, v_k) = \varepsilon_k^{g E_{n_k, v_k}} = 1 + g E_{n_k, v_k}^{(0)} \log(\varepsilon_k) + \frac{1}{2} g^2 (E_{n_k, v_k}^{(0)} \log(\varepsilon_k))^2 + g^2 E_{n_k, v_k}^{(1)} \log(\varepsilon_k) + \mathcal{O}(g^3), \quad (5.2)$$

where

$$E_{n_k, v_k} = \sum_{\ell=0}^{\infty} g^\ell E_{n_k, v_k}^{(\ell)} \quad (5.3)$$

is the expansion of the BFKL eigenvalue, the third term in (5.2) produces the first term in (5.1), whereas the fourth term in (5.2) produces the third term in (5.1). The first term in (5.1) constitutes the LLO part, the next three terms provide the NLL0 contribution, and the three terms on the second line form the NNLL0 piece.

⁹Since [24] analyzed the two-loop symbol for up to ten points, the equality has only been rigorously established for $n \leq 10$.

Passing now to the longer cut f_2 , one finds the following terms at three loops and leading logarithmic order:

$$\begin{aligned}
f_{2,(3)} &= \text{diagram 1} + \text{diagram 2} + \text{diagram 3} + \mathcal{O}(\text{NLLA}) \\
&= \text{diagram 4} + \text{diagram 5} + \text{diagram 6} + \mathcal{O}(\text{NLLA}). \quad (5.4)
\end{aligned}$$

As shown in the second line of this equation, two of the LLA diagrams can again be reduced to the six-point diagrams, using (4.3). But, unlike in the two-loop case, one LLA diagram remains that cannot be reproduced by six-point data. Removing the six-point pieces by subtracting two instances of $f_{1,(3)}$ functions, one finds the remainder

$$\begin{aligned}
g_3(\varepsilon_5, \varepsilon_6; w_5, w_6) &\equiv f_{2,(3)}(\varepsilon_5, \varepsilon_6; w_5, w_6) - f_{1,(3)}(\varepsilon_5; v_{5,6,5}) - f_{1,(3)}(\varepsilon_6; v_{5,6,6}) \\
&= \text{diagram 7} + \text{diagram 8} + \text{diagram 9} + \text{diagram 10} + \text{diagram 11} \\
&\quad - \text{diagram 12} - \text{diagram 13} + \text{diagram 14} + \text{diagram 15} + \text{diagram 16} \\
&\quad + \text{diagram 17} - \text{diagram 18} - \text{diagram 19} - \text{diagram 20} - \text{diagram 21}. \quad (5.5)
\end{aligned}$$

It is now straightforward to see that the general cut diagram $f_{k,(3)}$, to leading logarithmic order, becomes a sum of six-point functions $f_{1,(3)}$ and seven-point functions g_3 :¹⁰

$$\begin{aligned}
f_{k,(3)}^{\text{LLA}}(\varepsilon_5, \dots, \varepsilon_{4+k}; w_5, \dots, w_{4+k}) \\
&= \sum_{j=5}^{4+k} f_{1,(3)}^{\text{LLA}}(\varepsilon_j; v_{5,4+k;j}) + \sum_{i=5}^{3+k} \sum_{j=i+1}^{4+k} g_3^{\text{LLA}}(\varepsilon_i, \varepsilon_j; v_{5,j-1;i}, v_{i+1,4+k;j}). \quad (5.6)
\end{aligned}$$

Including all NNLO and NNLLO diagrams in the functions $f_{k,(3)}$, $f_{1,(3)}$, and g_3 on both sides of the above equation, and judiciously organizing all terms, one finds that the subleading contributions can be combined into two further NNLO building blocks g_L , g_R , and one further NNLLO building block h . The full three-loop cut function $f_{k,(3)}$ can be written as

$$\begin{aligned}
f_{k,(3)}(\varepsilon_5, \dots, \varepsilon_{k+4}; w_5, \dots, w_{k+4}) &= \sum_{j=5}^{k+4} f_{1,(3)}(\varepsilon_j; v_{5,4+k;j}) + \sum_{i=5}^{k+3} \sum_{j=i+1}^{k+4} g_3(\varepsilon_i, \varepsilon_j; v_{5,j-1;i}, v_{i+1,k+4;j}) \\
&+ \sum_{i=5}^{k+2} \sum_{j=i+1}^{k+3} g_L(\varepsilon_i; v_{5,j-1;i}, v_{i+1,j;j}, v_{j+1,k+4;j+1}) + \sum_{i=5}^{k+2} \sum_{j=i+2}^{k+4} g_R(\varepsilon_j; v_{5,i;i}, v_{i+1,j-1;i+1}, v_{i+2,k+4;j}) \\
&+ \sum_{i=5}^{k+1} \sum_{j=i+2}^{k+3} h(v_{5,i;i}, v_{i+1,j-1;i+1}, v_{i+2,j;j}, v_{j+1,k+4;j+1}). \quad (5.7)
\end{aligned}$$

The NNLO building block g_L depends on four intermediate momenta. It takes the form

$$g_L(\varepsilon_5; w_5, w_6, w_7) = \text{diagram 22} - \text{diagram 23} - \text{diagram 24} + \text{diagram 25}, \quad (5.8)$$

¹⁰Note that, contrary to the two-loop case (4.9), the three-loop building block g_3 is defined in terms of the original cross ratios w_5, w_6 rather than the combinations $v_{5,6,5}, v_{5,6,6}$.

and it gets summed over partitions of the sequence of momenta (p_4, \dots, p_{k+4}) into subsequences

$$(p_4, \dots, p_{i-1}), \quad (p_i, \dots, p_{j-1}), \quad (p_j), \quad \text{and} \quad (p_{j+1}, \dots, p_{k+4}). \quad (5.9)$$

The building block g_R is a mirror of g_L :

$$g_R(\varepsilon_7; w_5, w_6, w_7) = \begin{array}{c} \text{---} \\ | \quad | \quad | \\ \text{---} \\ | \quad | \quad | \\ \text{---} \end{array} - \begin{array}{c} \text{---} \\ \diagdown \quad | \quad | \\ \text{---} \\ | \quad | \quad | \\ \text{---} \end{array} - \begin{array}{c} \text{---} \\ | \quad \diagup \quad | \\ \text{---} \\ | \quad | \quad | \\ \text{---} \end{array} + \begin{array}{c} \text{---} \\ \diagdown \quad \diagup \quad | \\ \text{---} \\ | \quad | \quad | \\ \text{---} \end{array}, \quad (5.10)$$

and it gets summed over partitions into subsequences

$$(p_4, \dots, p_{i-1}), \quad (p_i), \quad (p_{i+1}, \dots, p_{j-1}), \quad \text{and} \quad (p_j, \dots, p_{k+4}). \quad (5.11)$$

Finally, the N^2 LLO building block h reads:

$$\begin{aligned} h(w_5, w_6, w_7, w_8) = & \begin{array}{c} \text{---} \\ | \quad | \quad | \quad | \\ \text{---} \\ | \quad | \quad | \quad | \\ \text{---} \end{array} - \begin{array}{c} \text{---} \\ \diagdown \quad | \quad | \quad | \\ \text{---} \\ | \quad | \quad | \quad | \\ \text{---} \end{array} - \begin{array}{c} \text{---} \\ | \quad \diagup \quad | \quad | \\ \text{---} \\ | \quad | \quad | \quad | \\ \text{---} \end{array} \\ + & \begin{array}{c} \text{---} \\ \diagdown \quad | \quad | \quad | \\ \text{---} \\ | \quad | \quad | \quad | \\ \text{---} \end{array} + \begin{array}{c} \text{---} \\ | \quad \diagdown \quad | \quad | \\ \text{---} \\ | \quad | \quad | \quad | \\ \text{---} \end{array} - \begin{array}{c} \text{---} \\ \diagdown \quad \diagdown \quad | \quad | \\ \text{---} \\ | \quad | \quad | \quad | \\ \text{---} \end{array} - \begin{array}{c} \text{---} \\ | \quad \diagdown \quad \diagdown \quad | \\ \text{---} \\ | \quad | \quad | \quad | \\ \text{---} \end{array} \\ - & \begin{array}{c} \text{---} \\ \diagdown \quad \diagup \quad | \quad | \\ \text{---} \\ | \quad | \quad | \quad | \\ \text{---} \end{array} - \begin{array}{c} \text{---} \\ | \quad \diagdown \quad \diagup \quad | \\ \text{---} \\ | \quad | \quad | \quad | \\ \text{---} \end{array} - \begin{array}{c} \text{---} \\ \diagdown \quad \diagup \quad \diagdown \quad | \\ \text{---} \\ | \quad | \quad | \quad | \\ \text{---} \end{array} + \begin{array}{c} \text{---} \\ \diagdown \quad \diagup \quad \diagup \quad | \\ \text{---} \\ | \quad | \quad | \quad | \\ \text{---} \end{array} \\ + & \begin{array}{c} \text{---} \\ \diagdown \quad \diagup \quad \diagdown \quad \diagdown \quad | \\ \text{---} \\ | \quad | \quad | \quad | \\ \text{---} \end{array} + \begin{array}{c} \text{---} \\ \diagdown \quad \diagup \quad \diagdown \quad \diagup \quad | \\ \text{---} \\ | \quad | \quad | \quad | \\ \text{---} \end{array} + \begin{array}{c} \text{---} \\ \diagdown \quad \diagup \quad \diagdown \quad \diagup \quad \diagdown \quad | \\ \text{---} \\ | \quad | \quad | \quad | \\ \text{---} \end{array} + \begin{array}{c} \text{---} \\ \diagdown \quad \diagup \quad \diagdown \quad \diagup \quad \diagup \quad | \\ \text{---} \\ | \quad | \quad | \quad | \\ \text{---} \end{array}. \quad (5.12) \end{aligned}$$

It gets summed over partitions of the intermediate momenta into subsequences

$$(p_4, \dots, p_{i-1}), \quad (p_i), \quad (p_{i+1}, \dots, p_{j-1}), \quad (p_j), \quad \text{and} \quad (p_{j+1}, \dots, p_{k+4}). \quad (5.13)$$

For the case $k = 3$, which is relevant for the eight-point remainder function, the last sum in the deconstruction (5.7) has to be replaced by the single term $\tilde{h}(w_5, w_6, w_7)$, where \tilde{h} is obtained from h (5.12) by removing the middle particle (and the associated LO emission vertex, where possible).

Using (3.5), equation (5.7) implies an analogous relation for the three-loop remainder function in the region $\rho = [4, n-1]$ where all intermediate momenta have been flipped:

$$\begin{aligned} R_{n,(3)}^{\text{MRL}}(\varepsilon_4, \dots, \varepsilon_{n-2}; w_4, \dots, w_{n-2}) \simeq & \sum_{j=5}^{n-1} R_{6,(3)}^{\text{MRL}}(\varepsilon_j; v_j) + \sum_{i=5}^{n-2} \sum_{j=i+1}^{n-1} g_3(\varepsilon_i, \varepsilon_j; v_{5,j-1;i}, v_{i+1,n-1;j}) \\ + & \sum_{i=5}^{n-3} \sum_{j=i+1}^{n-2} g_L(\varepsilon_i; v_{5,j-1;i}, v_{i+1,j;j}, v_{j+1,n-1;j+1}) + \sum_{i=5}^{n-3} \sum_{j=i+2}^{n-1} g_R(\varepsilon_j; v_{5,i;i}, v_{i+1,j-1;i+1}, v_{i+2,n-1;j}) \\ & + \sum_{i=5}^{n-4} \sum_{j=i+2}^{n-2} h(v_{5,i;i}, v_{i+1,j-1;i+1}, v_{i+2,j;j}, v_{j+1,k+4;j+1}). \quad (5.14) \end{aligned}$$

Here, the identities (4.16) have already been taken into account.

Note on the Alphabet. The three-loop three-particle building block $g_3(\varepsilon_5, \varepsilon_6; w_5, w_6)$ has the same alphabet \aleph (letters appearing in the entries of the symbol) as the two-loop three-particle building block $g_2(w_5, w_6)$:¹¹

$$\aleph = \{w_5, 1 + w_5, w_6, 1 + w_6, 1 + w_6 + w_5 w_6\}. \quad (5.15)$$

¹¹The full alphabet consists of \aleph and the complex conjugate set of letters $\bar{\aleph}$. It becomes more symmetric when switching to the variables $v_5 \equiv v_{5,6,5}$ and $v_6 \equiv v_{5,6,6}$, upon which $\aleph \rightarrow \{v_5, 1 + v_5, v_5 - v_6, v_6, 1 + v_6\}$. When replacing v_6 by $1/v_6$, it becomes fully symmetric, namely $\aleph \rightarrow \{v_5, 1 + v_5, v_6, 1 + v_6, 1 - v_5 v_6\}$.

Using the expansion (5.14), and expanding all variables $v_{k,l;j}$ in terms of w_5, \dots, w_{n-1} , the alphabet (of the terms in the first line) becomes big and complicated for larger n . Had one started with the n -point symbol, it would have been difficult to guess the variable transformation (4.11) that simplifies the alphabet and symbol terms.

Beyond seven points, the full alphabet of the remainder function remains unknown, even in the multi-Regge limit. At six and seven points, the alphabet apparently does not change with the loop order, with the full alphabet already visible at two loops. It appears likely that this pattern breaks at eight points, since this is the first instance at which the three-loop building blocks involve more independent legs than the two-loop building blocks. It would be interesting to work out the consequences of the deconstruction (5.14) on the higher-point alphabets in more detail.

6 Building Blocks

In principle, each term in the perturbative expansion of the Regge cut diagram (3.5) can be computed from the integral representation (2.28), once the expressions for the BFKL eigenvalue, impact factor, and central emission vertex are known to the desired perturbative order. In the previous sections, we have shown that, by judiciously organizing all terms in the expansion, the n -point two-loop and three-loop cut contributions can be reconstructed from a few basic building blocks that are functions of the anharmonic ratios w_j . Once these building block functions are known, the Regge cut contribution to the remainder function can be computed via the formula (4.14,5.14).

Here, we will content ourselves with treating the relevant functions at the level of the symbol. The symbol of the two-loop NLL0 building block $g_2(v_1, v_2)$ has been obtained [24] by taking the multi-Regge limit of the known two-loop remainder function symbol [25] and using the decomposition (4.15).

At three-loop order, we have the six-point [35] and seven-point [17] remainder function symbols at our disposal. By definition, this data is sufficient to extract the symbol of the LLA building block g_3 (5.5). Applying in turn the first line of the three-loop decomposition (5.14), this admits a reconstruction of the n -point remainder function symbol at leading logarithmic order.

We compute the multi-Regge limit symbol of the three-loop remainder function in the same way as for the two-loop symbol. The procedure is detailed in [24], here we only give a brief summary: Starting with the known six-point [35] and seven-point [17] symbols for general kinematics, we expand all first entries in terms of the cross ratios (2.10) via the symbol rule

$$(xy) \otimes (z) = (x) \otimes (z) + (y) \otimes (z). \quad (6.1)$$

Next, we collect all terms with the same cross ratio $u_{k,i}$ in the first entry, strip off the first entry, and multiply by $2\pi i$. The result is the symbol of the discontinuity under continuation along the path $u_{k,i} \rightarrow e^{2\pi i} u_{k,i}$. We obtain the multi-Regge limit of each such discontinuity by expressing the kinematic invariants in the symbol entries by the OPE variables

$$\{T_j, S_j, F_j\} = \{e^{-\tau_j}, e^{\sigma_j}, e^{i\phi_j}\}, \quad j = 5, \dots, n-1, \quad (6.2)$$

of [14], setting $S_j = T_j / \sqrt{w_j \bar{w}_j}$ and $F_j = \sqrt{w_j / \bar{w}_j}$, and by taking the limit $T_j \rightarrow 0$, keeping only the leading term in each entry. Next, setting $T_j = (\varepsilon_j^2 w_j \bar{w}_j)^{1/4}$, and again expanding all terms via (6.1), one can finally extract all large logarithms via the shuffle relations

$$\begin{aligned} \log(\varepsilon_j)(x \otimes y \otimes \dots \otimes z) &= (\varepsilon_j \otimes x \otimes y \otimes \dots \otimes z) + (x \otimes \varepsilon_j \otimes y \otimes \dots \otimes z) \\ &+ (x \otimes y \otimes \varepsilon_j \otimes \dots \otimes z) + \dots + (x \otimes y \otimes \dots \otimes \varepsilon_j \otimes z) + (x \otimes y \otimes \dots \otimes z \otimes \varepsilon_j). \end{aligned} \quad (6.3)$$

At seven points and three loops, the resulting expression for each discontinuity is a degree-two polynomial in $\log(\varepsilon_5)$ and $\log(\varepsilon_6)$, whose coefficients are symbols with five entries that exclusively depend on w_5 , w_6 , and their complex conjugates. Starting in the kinematic region $(---)$ in which no intermediate momentum is flipped, each other kinematic region is associated with specific winding numbers for all cross ratios $u_{k,i}$. Summing the corresponding discontinuities then yields the remainder function in the respective kinematic region. In particular, the region $(+++)$ that contains the three-particle cut f_2 , only the cross-ratio $U_{2,6}$ (2.8) winds non-trivially. Applying the change of variables (4.5,4.6) and subtracting the respective six-point three-loop symbols (5.5), one finally obtains the symbol of the building block g_3 .

The NNLO and N²LLA building blocks (5.8,5.10,5.12) first appear in the three-loop eight-point and nine-point amplitudes, and can thus not (yet) be extracted from available data. In principle these functions could be computed term by term from the integral representation (2.28). While the BFKL eigenvalue and impact factor are known explicitly to N²LLA and N³LLA [7, 9, 16, 36], and all order expressions have been proposed [37], the missing ingredient is the NLO and NNLO central emission vertex (2.25).

In principle, the NLO emission vertex could be extracted from the building block g_2 by subtracting the two reducible terms and inverting the Fourier–Mellin transform. This however requires knowledge of the full function g_2 , which at present is only known at leading transcendental weight [24].

The attached MATHEMATICA file `MRL3LLA.m` contains the symbols for the building blocks $R_{6,(3)}^{\text{MRL}}$ and g_3 , as well as a function that reconstructs the three-loop leading-logarithmic-order remainder function symbol from these building blocks.

7 Conclusion

Summary. A central result of this work is the relation (5.14), which expresses the simplest cut contribution to the n -point remainder function at three loops in terms of a few basic building blocks. It should be emphasized that the identity has a two-fold meaning: On the one hand, it holds at the level of the remainder function *symbol*. On the other hand, it holds at the level of full *functions* once one restricts the remainder function to its simplest cut contribution as in (3.5), neglecting the Regge pole terms as well as higher Regge cut contributions such as the ones in the last line of (2.23).

The second main result is the determination of the three-loop building block g_3 at the level of the symbol from the known seven-point three-loop symbol for general kinematics [17]. Together with the symbol of the known six-point building block [35], this permits the reconstruction of the three-loop remainder function symbol at leading logarithmic order, as implemented in the attached MATHEMATICA file.

Outlook. It would be interesting to better understand the general relation between the BFKL building blocks—impact factors, eigenvalues, and emission vertices—and the perturbative building blocks that we found for the full cut contributions. Of course, this relation is in principle provided by the Fourier–Mellin transform. However, the action of the inverse Fourier–Mellin transform on general expressions of multiple polylogs is (to the author’s knowledge) not understood systematically. Especially, it would be interesting to understand how much can be learnt about the BFKL building blocks when the cut contributions are only known at the symbol level. A better understanding of this point would admit to extract the NLO emission vertex from two-loop data, from which the three-loop NLO building blocks g_L and g_R could then be constructed.

We have only determined the three-loop six-point and seven-point building blocks at the level of their symbols. That is, we have discarded all information about terms of lower functional transcendentality. Acquiring the full building block *functions* would require to reconstruct those lower-weight terms, for example by imposing physical symmetry and analyticity constraints, or by comparison with the collinear limit. However, constructing the multi-Regge limit remainder function at subleading functional transcendentality also requires to take more general multi-Reggeon cut terms into account, such as the ones shown in the last line of (2.23). While it might be possible to project out such terms by selecting specific kinematic regions, these higher cut terms form an interesting subject on their own that remains largely unexplored to date.

An interesting and promising approach to understanding multi-Regge limit amplitudes is the integrability-based Wilson loop OPE [13]. By an ingenious analytic continuation, the full all-loop cut term f_1 could be extracted from the six-point OPE [37]. While difficult, it is conceivable that further cut terms can be obtained in a similar way.

Acknowledgments

I sincerely wish to thank Jochen Bartels for many very instructive and enjoyable discussions, as well as for comments on the manuscript. I also want to thank Johannes Brödel, Vsevolod Chestnov, Volker Schomerus, and Martin Sprenger for valuable discussions. My work is supported by a Marie Curie International Outgoing Fellowship within the 7th European Community Framework Programme under Grant No. PIOF-GA-2011-299865.

References

- [1] V. S. Fadin, E. A. Kuraev and L. N. Lipatov, “On the Pomeron Singularity in Asymptotically Free Theories”, Phys. Lett. B60, 50 (1975). ★ E. A. Kuraev, L. N. Lipatov and V. S. Fadin, “Multi-Reggeon Processes in the Yang–Mills Theory”, Sov. Phys. JETP 44, 443 (1976). ★ I. I. Balitsky and L. N. Lipatov, “The Pomeron Singularity in Quantum Chromodynamics”, Sov. J. Nucl. Phys. 28, 822 (1978).
- [2] J. Bartels, “High-Energy Behavior in a Nonabelian Gauge Theory. 2. First Corrections to $T(n \rightarrow m)$ Beyond the Leading LNS Approximation”, Nucl. Phys. B175, 365 (1980). ★ J. Kwieciński and M. Praszalowicz, “Three Gluon Integral Equation and Odd c Singlet Regge Singularities in QCD”, Phys. Lett. B94, 413 (1980).
- [3] N. Beisert et al., “Review of AdS/CFT Integrability: An Overview”, Lett. Math. Phys. 99, 3 (2012), arxiv:1012.3982.
- [4] Z. Bern, L. J. Dixon and V. A. Smirnov, “Iteration of planar amplitudes in maximally supersymmetric Yang–Mills theory at three loops and beyond”, Phys. Rev. D72, 085001 (2005), hep-th/0505205.
- [5] L. F. Alday and J. Maldacena, “Comments on gluon scattering amplitudes via AdS/CFT”, JHEP 0711, 068 (2007), arxiv:0710.1060.
- [6] J. Bartels, L. N. Lipatov and A. Sabio Vera, “BFKL Pomeron, Reggeized gluons and Bern-Dixon-Smirnov amplitudes”, Phys. Rev. D80, 045002 (2009), arxiv:0802.2065.
- [7] J. Bartels, L. N. Lipatov and A. Sabio Vera, “ $\mathcal{N} = 4$ supersymmetric Yang Mills scattering amplitudes at high energies: The Regge cut contribution”, Eur. Phys. J. C65, 587 (2010), arxiv:0807.0894.
- [8] L. N. Lipatov, “Analytic properties of high energy production amplitudes in $\mathcal{N} = 4$ SUSY”, Theor. Math. Phys. 170, 166 (2012), arxiv:1008.1015.
- [9] L. J. Dixon, J. M. Drummond, C. Duhr and J. Pennington, “The four-loop remainder function and multi-Regge behavior at NNLLA in planar $\mathcal{N} = 4$ super-Yang–Mills theory”, JHEP 1406, 116 (2014), arxiv:1402.3300.

- [10] L. J. Dixon, M. von Hippel and A. J. McLeod, “*The four-loop six-gluon NMHV ratio function*”, JHEP 1601, 053 (2016), arxiv:1509.08127.
- [11] A. B. Goncharov, “*Multiple polylogarithms and mixed Tate motives*”, math/0103059.
★ F. C. S. Brown, “*Polylogarithmes multiples uniformes en une variable*”, Comptes Rendus Mathematique 338, 527 (2004),
<http://www.sciencedirect.com/science/article/pii/S1631073X04000780>.
- [12] S. Caron-Huot and S. He, “*Jumpstarting the All-Loop S-Matrix of Planar $\mathcal{N} = 4$ Super Yang–Mills*”, JHEP 1207, 174 (2012), arxiv:1112.1060.
- [13] B. Basso, A. Sever and P. Vieira, “*Spacetime and Flux Tube S-Matrices at Finite Coupling for $\mathcal{N} = 4$ Supersymmetric Yang–Mills Theory*”, Phys. Rev. Lett. 111, 091602 (2013), arxiv:1303.1396.
- [14] B. Basso, A. Sever and P. Vieira, “*Space-time S-matrix and Flux tube S-matrix II. Extracting and Matching Data*”, JHEP 1401, 008 (2014), arxiv:1306.2058.
- [15] L. J. Dixon, C. Duhr and J. Pennington, “*Single-valued harmonic polylogarithms and the multi-Regge limit*”, JHEP 1210, 074 (2012), arxiv:1207.0186.
- [16] L. J. Dixon, J. M. Drummond, M. von Hippel and J. Pennington, “*Hexagon functions and the three-loop remainder function*”, JHEP 1312, 049 (2013), arxiv:1308.2276.
- [17] J. M. Drummond, G. Papathanasiou and M. Spradlin, “*A Symbol of Uniqueness: The Cluster Bootstrap for the 3-Loop MHV Heptagon*”, JHEP 1503, 072 (2015), arxiv:1412.3763.
- [18] J. Bartels, L. N. Lipatov and A. Prygarin, “*Collinear and Regge behavior of $2 \rightarrow 4$ MHV amplitude in $\mathcal{N} = 4$ super Yang–Mills theory*”, arxiv:1104.4709.
- [19] J. Bartels, A. Kormilitzin, L. N. Lipatov and A. Prygarin, “*BFKL approach and $2 \rightarrow 5$ maximally helicity violating amplitude in $\mathcal{N} = 4$ super-Yang–Mills theory*”, Phys. Rev. D86, 065026 (2012), arxiv:1112.6366.
- [20] J. Bartels, A. Kormilitzin and L. Lipatov, “*Analytic structure of the $n = 7$ scattering amplitude in $\mathcal{N} = 4$ SYM theory in the multi-Regge kinematics: Conformal Regge pole contribution*”, Phys. Rev. D89, 065002 (2014), arxiv:1311.2061.
- [21] J. Bartels, A. Kormilitzin and L. N. Lipatov, “*Analytic structure of the $n = 7$ scattering amplitude in $\mathcal{N} = 4$ theory in multi-Regge kinematics: Conformal Regge cut contribution*”, Phys. Rev. D91, 045005 (2015), arxiv:1411.2294.
- [22] J. Bartels, V. Schomerus and M. Sprenger, “*Multi-Regge Limit of the n -Gluon Bubble Ansatz*”, JHEP 1211, 145 (2012), arxiv:1207.4204.
- [23] J. Bartels, V. Schomerus and M. Sprenger, “*The Bethe roots of Regge cuts in strongly coupled $\mathcal{N} = 4$ SYM theory*”, JHEP 1507, 098 (2015), arxiv:1411.2594.
- [24] T. Bargheer, G. Papathanasiou and V. Schomerus, “*The Two-Loop Symbol of all Multi-Regge Regions*”, JHEP 1605, 012 (2016), arxiv:1512.07620.
- [25] S. Caron-Huot, “*Superconformal symmetry and two-loop amplitudes in planar $\mathcal{N} = 4$ super Yang–Mills*”, JHEP 1112, 066 (2011), arxiv:1105.5606.
- [26] T. Regge, “*Bound states, shadow states and Mandelstam representation*”, Nuovo Cim. 18, 947 (1960).
- [27] D. Amati, A. Stanghellini and S. Fubini, “*Theory of high-energy scattering and multiple production*”, Nuovo Cim. 26, 896 (1962).
- [28] S. Mandelstam, “*Cuts in the Angular Momentum Plane. 2*”, Nuovo Cim. 30, 1148 (1963).
- [29] “*The On-Line Encyclopedia of Integer Sequences*”, published electronically, <https://oeis.org>.
- [30] J. Bartels, to appear.
- [31] L. N. Lipatov, “*Integrability of scattering amplitudes in $N=4$ SUSY*”, J. Phys. A42, 304020 (2009), arxiv:0902.1444.
- [32] S. Caron-Huot and K. J. Larsen, “*Uniqueness of two-loop master contours*”, JHEP 1210, 026 (2012), arxiv:1205.0801.

- [33] A. B. Goncharov, “A simple construction of Grassmannian polylogarithms”, arxiv:0908.2238.
★ C. Duhr, H. Gangl and J. R. Rhodes, “From polygons and symbols to polylogarithmic functions”,
JHEP 1210, 075 (2012), arxiv:1110.0458. ★ C. Duhr, “Mathematical aspects of scattering
amplitudes”, arxiv:1411.7538, in: “Theoretical Advanced Study Institute in Elementary Particle
Physics: Journeys Through the Precision Frontier: Amplitudes for Colliders (TASI 2014) Boulder,
Colorado, June 2-27, 2014”.
- [34] A. Prygarin, M. Spradlin, C. Vergu and A. Volovich, “All Two-Loop MHV Amplitudes in
Multi-Regge Kinematics From Applied Symbology”, Phys. Rev. D85, 085019 (2012),
arxiv:1112.6365.
- [35] L. J. Dixon, J. M. Drummond and J. M. Henn, “Bootstrapping the three-loop hexagon”,
JHEP 1111, 023 (2011), arxiv:1108.4461.
- [36] V. S. Fadin and L. N. Lipatov, “BFKL equation for the adjoint representation of the gauge group in the
next-to-leading approximation at $\mathcal{N} = 4$ SUSY”, Phys. Lett. B706, 470 (2012), arxiv:1111.0782.
★ L. N. Lipatov and A. Prygarin, “BFKL approach and six-particle MHV amplitude in $\mathcal{N} = 4$ super
Yang–Mills”, Phys. Rev. D83, 125001 (2011), arxiv:1011.2673.
- [37] B. Basso, S. Caron-Huot and A. Sever, “Adjoint BFKL at finite coupling: a short-cut from the
collinear limit”, JHEP 1501, 027 (2015), arxiv:1407.3766.